Replication and trafficking of a plant virus are coupled at the entrances of plasmodesmata

Jens Tilsner,[1,2,3] Olga Linnik,[3] Marion Louveaux,[3] Ian M. Roberts,[2] Sean N. Chapman,[2] and Karl J. Oparka[3]

[1]Biomedical Sciences Research Complex, University of St Andrews, Fife KY16 9ST, Scotland, UK
[2]Cell and Molecular Sciences, The James Hutton Institute, Dundee DD2 5DA, Scotland, UK
[3]Institute of Molecular Plant Sciences, University of Edinburgh, Edinburgh EH9 3JR, Scotland, UK

Plant viruses use movement proteins (MPs) to modify intercellular pores called plasmodesmata (PD) to cross the plant cell wall. Many viruses encode a conserved set of three MPs, known as the triple gene block (TGB), typified by Potato virus X (PVX). In this paper, using live-cell imaging of viral RNA (vRNA) and virus-encoded proteins, we show that the TGB proteins have distinct functions during movement. TGB2 and TGB3 established endoplasmic reticulum–derived membranous caps at PD orifices. These caps harbored the PVX replicase and nonencapsidated vRNA and represented PD-anchored viral replication sites. TGB1 mediated insertion of the viral coat protein into PD, probably by its interaction with the 5′ end of nascent virions, and was recruited to PD by the TGB2/3 complex. We propose a new model of plant virus movement, which we term coreplicational insertion, in which MPs function to compartmentalize replication complexes at PD for localized RNA synthesis and directional trafficking of the virus between cells.

Introduction

Viruses must transport their genomes between host cells to continue their infection. In plants, the cell wall blocks potential transport by endocytic mechanisms. Plant viruses therefore move through plasmodesmata (PD), plant-specific intercellular nanopores that connect the plasma membrane, cytoplasm, and ER through the cell wall (Tilsner et al., 2011). Viral transport is mediated by one or several virus-encoded movement proteins (MPs) that target and move through PD, dilate the PD pore (gating), and bind nucleic acids nonsequence specifically (Lucas, 2006). Plant virus movement is a prime target for development of new crop protection strategies because the number of transported viral genomes is extremely small, in the order of units (Gutiérrez et al., 2012). However, despite intense research efforts, the key steps in virus movement remain elusive at the molecular level.

Potato virus X (PVX) is an economically important plant virus that finds wide use as a silencing and expression vector and also serves as a model system for RNA silencing and plant immune responses as well as virus movement (Verchot-Lubicz et al., 2007). It typifies plant viruses encoding three MPs in overlapping ORFs, the triple gene block (TGB; Fig. 1), a genetic module conserved in several plant virus families (Morozov and Solovyev, 2003; Verchot-Lubicz et al., 2010). All three TGB proteins, as well as the capsid protein (CP), are required for PVX movement.

TGB1, encoded by the first ORF, is an RNA helicase (Kalinina et al., 2002), a suppressor of RNA silencing (Voinnet et al., 2000), and a translational activator (Atabekov et al., 2000). Specific interaction of TGB1 with CP subunits at the 5′ end of wholly or partially encapsidated virions destabilizes the virus coat, enabling ribosomal access (Atabekov et al., 2000; Rodionova et al., 2003). Because CP is required for movement and has been detected within PD of infected tissue (Chapman et al., 1992; Oparka et al., 1996; Santa Cruz et al., 1998), the transport form of PVX may consist of partially encapsidated viral RNA (vRNA) with 5′-associated TGB1 (Verchot-Lubicz

Correspondence to Jens Tilsner: jt58@st-andrews.ac.uk

M. Louveaux's present address is Laboratoire Reproduction et Développement des Plantes, UMR 5667, Ecole Normale Supérieure de Lyon, 69364 Lyon, Cedex 07, France.

Abbreviations used in this paper: 3D-SIM, 3D structured illumination microscopy; CP, capsid protein; dpi, day postinfiltration; FP, fluorescent protein; MP, movement protein; PD, plasmodesmata; PUM-BiFC, Pumilio-coupled bimolecular fluorescence complementation; PVX, Potato virus X; TEM, transmission EM; TGB, triple gene block; TMV, Tobacco mosaic virus; VRC, viral replication complex; vRNA, viral RNA.

The Rockefeller University Press $30.00
J. Cell Biol. Vol. 201 No. 7 981–995
www.jcb.org/cgi/doi/10.1083/jcb.201304003

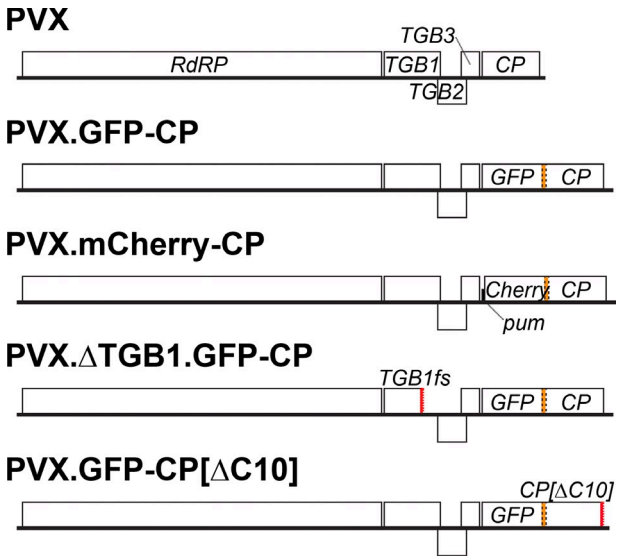

Figure 1. **PVX genome and modified viruses used in this study.** Shown to scale. *RdRP*: RNA-dependent RNA polymerase (replicase). In the *GFP-* and *mCherry-CP* fusions, the orange dashed box indicates the presence of a partially self-cleaving linker peptide (Santa Cruz et al., 1996). *pum*: tag for vRNA detection using PUM-BiFC (Tilsner et al., 2009). *TGB1fs*: +1 frameshift after 153 codons (dashed red box indicates translated missense codons). *CP[ΔC10]*: 10 C-terminal codons deleted (dashed red box).

et al., 2010). Though TGB1 gates PD and localizes to them in infected cells (Howard et al., 2004; Samuels et al., 2007), it does not target PD itself. Likely, TGB1 is recruited to PD by the other two TGB proteins similar to other TGB-encoding viruses (Erhardt et al., 2000; Verchot-Lubicz et al., 2010), although for PVX this has not been shown directly.

The two TGB proteins encoded by the middle and last ORFs (TGB2 and 3) are small transmembrane proteins that colocalize in ER-derived granules induced by TGB2 (Krishnamurthy et al., 2003; Ju et al., 2005; Samuels et al., 2007) and in peripheral bodies formed by TGB3 (Schepetilnikov et al., 2005; Lee et al., 2010). The TGB2 and 3 proteins form heterologous interactions (Lee et al., 2010), and TGB3 is generally viewed as the PD targeting factor (Solovyev et al., 2000; Schepetilnikov et al., 2005; Lee et al., 2010; Wu et al., 2011). However, it remains unclear how the individual TGB proteins and CP contribute to movement.

Another open question is where in the cell do viral MPs pick up their vRNA cargo for transport (Tilsner and Oparka, 2012)? Current models borrow heavily from animal virus literature in which intracellular replication complexes are discrete structures associated with host membranes (den Boon et al., 2010) and commonly assume that progeny vRNA is transported from such sites to the cell periphery, i.e., that replication and movement are spatially separated processes (Lucas, 2006; Verchot-Lubicz et al., 2010; Schoelz et al., 2011). PVX replicates in association with ER membranes (Doronin and Hemenway, 1996), and the 165k (165 kD) RNA-dependent RNA polymerase (replicase) colocalizes with the ER-derived TGB2/3 granules (Bamunusinghe et al., 2009). We recently found that the TGB proteins collectively organize a perinuclear viral replication complex (VRC) at late infection stages (Tilsner et al., 2012; Linnik et al., 2013). Because the TGB proteins are dispensable for replication (Morozov and Solovyev, 2003), we hypothesized that their interaction with replication sites might be related to their movement function.

Here, we show that the TGB proteins have distinct localizations at PD that are related to their specific functions during movement. TGB2 and 3 remodel ER membranes at the PD orifice into "caps" that harbor the replicase and vRNA. TGB1 is recruited by the TGB2/3 complex and accumulates within the pores. It is responsible for the deposition of CP, probably incorporated into virions, inside PD. We propose a new model of PVX movement, coreplicational insertion, in which vRNA processing and trafficking are highly compartmentalized at PD, revealing a mechanism that may be a widespread feature of plant virus infections.

Results

The TGB proteins have distinct subplasmodesmal localizations

To clarify the roles of the TGB proteins during PVX movement, we analyzed their distribution in the context of infection, using viruses expressing fluorescent protein (FP)–CP fusions (Fig. 1). The fluorescent CP is incorporated into functional virions and accumulates in PD and thus served as a marker for PD targeting and virus transport (Santa Cruz et al., 1996, 1998). The FP-CP fusions also allowed us to follow the spread of viral lesions across the leaf lamina. The leading edge of the lesions represents the most recently infected cells, where movement occurs. To circumvent problems with multiply tagged viruses and fusions that disrupted the overlapping TGB ORFs, FP-fused viral proteins were expressed ectopically by infiltrating leaves with agrobacteria carrying suitable expression constructs. When virus lesions entered these agropatches, protein localizations could be observed in the context of viral infection (and also in the presence of the corresponding unfused protein expressed from the viral genome).

In infected cells overlapping with agropatches that expressed TGB1 fusions, TGB1 localized to PD (Fig. 2, A–C), as previously observed when GFP-TGB1 was overexpressed from a modified virus (Samuels et al., 2007). The PD localization was consistent throughout infection sites, irrespective of whether N- or C-terminal FP fusions were used (both fusions have been reported previously to complement virus movement; Howard et al., 2004; Bayne et al., 2005). At higher magnification, TGB1 colocalized precisely with CP inside the PD channel within the intercellular wall space (Fig. 2, B and C).

FP-TGB2, which also complements movement (Ju et al., 2005), localized to PD when PVX lesions entered the agropatches (Fig. 2, D–G). In contrast to TGB1, however, TGB2 did not colocalize with CP but rather was found in punctate caps at the cytoplasmic orifices of PD, aligning with the CP inside the pores (Fig. 2 E). Only occasionally, in cells near the infection front, was TGB2 also observed within CP-labeled PD channels (Fig. 2 F). This observation was confirmed by immunogold EM on PVX-infected tissue using an antibody raised against

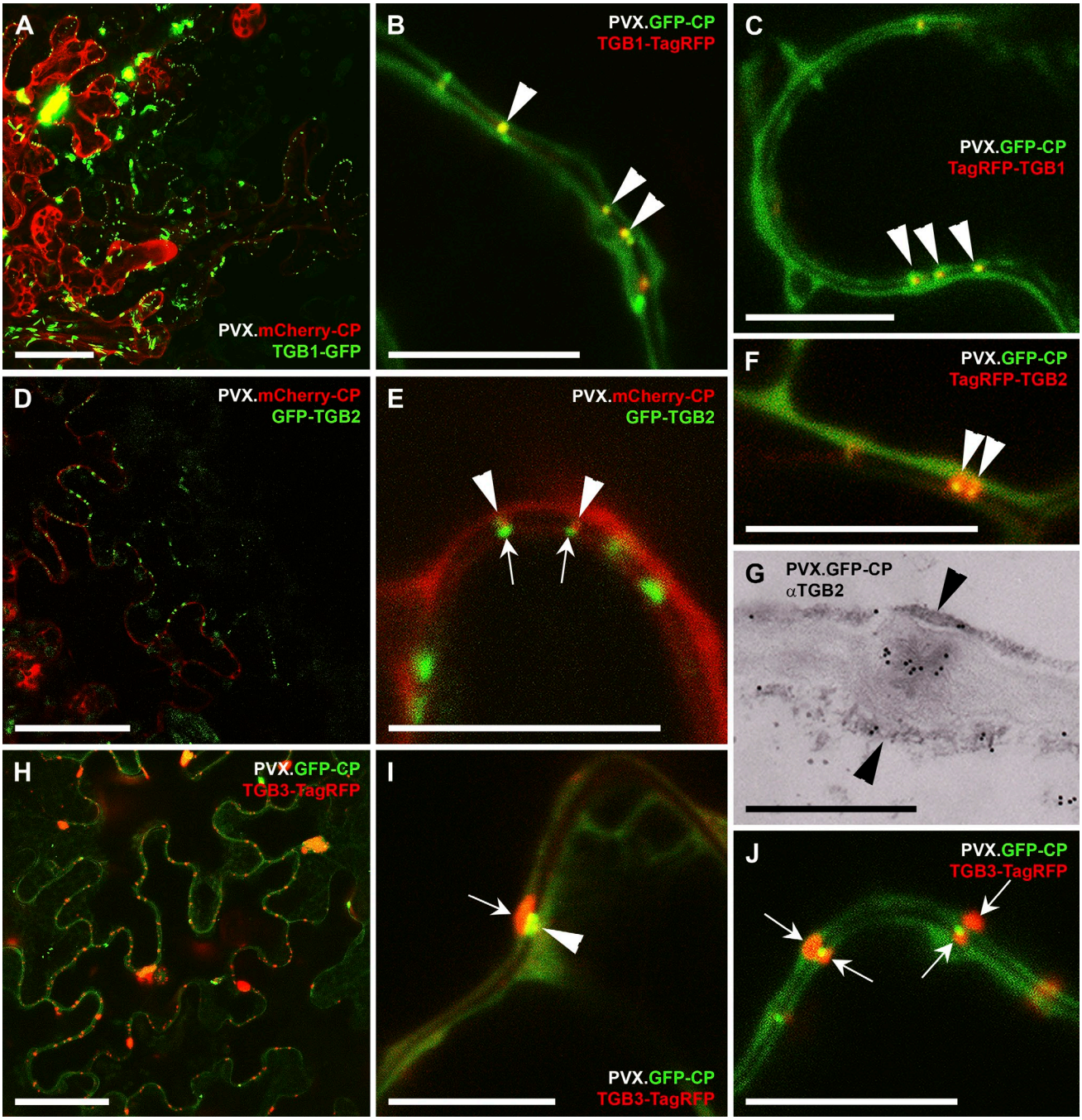

Figure 2. **Distinct subplasmodesmal localizations of the TGB proteins.** (A) TGB1-GFP at the leading edge of infection. (B and C) Both TGB1-TagRFP and TagRFP-TGB1 are located inside PD channels (arrowheads) together with GFP-CP. The dark area between cytoplasms of adjacent cells (faintly labeled by GFP-CP) is the cell wall. (D) GFP-TGB2 at the leading edge of infection. (E) GFP-TGB2 resides in caps (arrows) aligned with mCherry-CP–labeled PD (arrowheads). (F) TagRFP-TGB2 colocalized with GFP-CP within the PD channel (arrowheads). (G) Immunogold labeling of the PD cavity with antibodies against TGB2 (arrowheads: PD orifices). Gold particles are also associated with cortical ER appressed to the cell periphery. (H) TGB3-TagRFP two to three cells behind the infection front. (I) TGB3-TagRFP in caps (arrows in I and J) at the PD orifice, aligning with GFP-CP embedded in the PD pore within the cell wall (arrowhead). (J) Caps often occur on both sides of PD. All confocal images are individual z sections except A and H, which are maximum projections of entire z stacks. Bars: (A, D, and H) 50 µm; (B, C, E, F, I, and J) 10 µm; (G) 500 nm.

TGB2, which labeled the central cavities inside PD (Fig. 2 G). As TGB2 localizes to ER membranes (Ju et al., 2005), which are extremely constricted within PD (Tilsner et al., 2011), it is possible that the FP-TGB2 signal originating from within the pores is generally not strong enough to be detectable by confocal microscopy.

TGB3-FP, which complements movement (Schepetilnikov et al., 2005; Samuels et al., 2007), was also found in caps at the PD orifices (Fig. 2, H–J). Caps were often seen on both sides of PD (Fig. 2 J). Thus, all three TGB proteins are localized to PD during PVX infection but accumulate at distinct areas of PD: TGB1 inside the pores together with CP and TGB2/3 in caps at the PD orifices.

The PD caps also contain replicase and nonencapsidated vRNA

Because ER-derived TGB2/3 granules are associated with PVX replicase, virions, and ribosomes (Ju et al., 2005; Bamunusinghe et al., 2009), we hypothesized that the caps could be PD-anchored replication sites. FP fusions of the complete replicase produced only very weak fluorescence (unpublished data). However, a C-terminally truncated replicase consisting of only the methyltransferase and RNA helicase domains (165k$^{[1–997]}$-GFP) produced sufficient fluorescence to allow imaging in the presence of PVX.mCherry-CP. At the leading edge of infection, the replicase was found in punctae aligned with PD that contained mCherry-CP (Fig. 3, A and B). In cells immediately behind the infection front, the replicase fusion gave a granular labeling of the larger PD caps (Fig. 3, E, F, and H) and was also present in VRCs, arranged in identical "whorls" to those described previously for vRNA (Fig. 3, I and K; Tilsner et al., 2009, 2012). In uninfected cells, the replicase fusion formed aggregates in the nucleoplasm (Fig. 3 L). Coexpression of all TGB proteins and CP did not change this replicase localization, and no 165k$^{[1–997]}$-GFP was observed in TGB3-TagRFP–labeled caps at PD (Fig. 3, M and N). Thus, the recruitment of replicase to PD caps required the context of a complete PVX infection.

We next imaged nonencapsidated vRNA in vivo, using modified variants of the sequence-specific, single-stranded RNA binding domain of human Pumilio1 coupled to bimolecular fluorescence complementation (PUM-BiFC; Tilsner et al., 2009, 2012). PUM-BiFC fluorescence was concentrated in small punctae adjacent to mCherry-CP–labeled PD at the leading edge of infection (Fig. 3, C and D) and also in granular punctae within larger PD caps (Fig. 3 G). The largest caps showed vRNA whorls (Fig. 3, J and K) like those previously observed in VRCs (Tilsner et al., 2009, 2012). Because the PUM-BiFC reporter does not label encapsidated virions (Tilsner et al., 2009, 2012), there is thus a pool of nonencapsidated vRNA present in the PD caps. Combined with the replicase localization we observed, our data strongly indicate that the caps are replication sites. As PVX probably moves at least partially encapsidated (Santa Cruz et al., 1998), the inability of PUM-BiFC to label vRNA within PVX virions most likely explains why the PUM-BiFC signal was not detected inside PD as well.

TGB2 and 3 both target PD and jointly recruit TGB1

To dissect the individual functions of the TGB proteins, we first attempted to identify the PD targeting factor by localizing each TGB protein in the absence of virus. We tested only those FP fusions that complemented movement. All TGB proteins form homo-oligomers (Leshchiner et al., 2008; Tseng et al., 2009; Wu et al., 2011). Because coexpressed unfused protein may rescue targeting of FP fusions (Schepetilnikov et al., 2005), we additionally tested all FP fusions with coexpressed unfused protein (Table S1). We also began analysis of TGB localizations at 1 d postinfiltration (dpi) to observe them at the lowest detectable expression levels.

Neither N- nor C-terminal fusions of TGB1 localized to PD in the presence or absence of additional unfused TGB1 (Fig. S1, A–E), confirming that this protein does not target PD by itself. TGB2 has previously been observed in the tubular ER network and ER-derived granules (Ju et al., 2005). After 2–3 dpi, we observed this phenotype in all cells expressing GFP-TGB2 (Fig. 4 B). However, at 1–2 dpi, in cells with low expression levels, GFP-TGB2 fluorescence in the tubular ER was extremely faint and the only part of the ER that was strongly labeled was the nuclear envelope (Fig. 4 A). At this stage, very few ER-associated granules were observed. Instead, GFP-TGB2 fluorescence was concentrated in punctae that were located almost exclusively along the lateral walls where PD were present (Fig. 4 A). Costaining with the PD marker aniline blue, which labels the callose present at PD, confirmed that the peripheral TGB2 punctae were localized in PD caps (Fig. 4 C). Coexpression of unfused TGB2 did not alter this localization (Table S1). Quantitative analysis of GFP-TGB2 distribution from the earliest time point at which GFP fluorescence was detected revealed that at 21 h after infiltration, 100% of cells (n = 23) showed only PD labeling. At 28 h after infiltration, 40.8% of cells (n = 142) had GFP-TGB2 concentrated in PD, whereas in 59.2% of cells the ER network and ER-associated granules were labeled. After 2 dpi, GFP-TGB2 labeled the ER and granules in all cells. Hence, TGB2 targets PD first, before inducing the formation of ER-associated granules.

TGB3-FP fusions localized to the tubular ER network and cytoplasm but neither formed granules nor localized to PD (Fig. S2, A and B). However, coexpression of unfused TGB3 led to the formation of small motile punctae on the cortical ER, and in some cells, these were slightly enlarged along the cell periphery (Fig. 4 D). Aniline blue staining showed that these peripheral punctae were PD caps. These results confirm that unfused TGB3 is required for the formation of PD caps (see also Schepetilnikov et al., 2005). Because TGB2 and 3 probably act as a complex (Lee et al., 2010), we also tested the influence of TGB2 on the ability of TGB3 to localize to PD. Coexpression of unfused TGB2 resulted in a marked increase in TGB3-FP–labeled caps (Fig. 4 E and Table S1). Thus, TGB2 increases PD targeting of TGB3-FP.

Because PVX TGB1 does not target PD, we next tested whether it is recruited there by TGB2 and 3, as is the case for other TGB viruses (Erhardt et al., 2000; Verchot-Lubicz et al., 2010). Both FP-TGB1 and TGB1-FP fusions became localized to PD when each fusion protein was coexpressed with unfused TGB2 and 3 (Fig. 4, F–H). In TGB1-FP coexpressions with TGB2 and 3, 99.4% of cells showed PD labeling (n = 303). When TGB1 fusions were coexpressed with TGB2 or TGB3 alone, no PD localization was observed (0%, n = 100 cells each), showing that both TGB2 and TGB3 are required for TGB1 recruitment (Fig. S1, F–I). Recruitment of TGB1 to PD by TGB2/3 in almost all cells, but not by either protein alone, proves that the unfused proteins were expressed and functional and that the large majority of cells received all three expression constructs. In a natural PVX infection, TGB2 and 3 are coexpressed from a bicistronic messenger RNA at a ratio of ∼10:1 (Verchot-Lubicz et al., 2010). However, we did not observe an effect of the TGB2/3 ratio on TGB1 recruitment (Fig. 4, F and G; and Table S1).

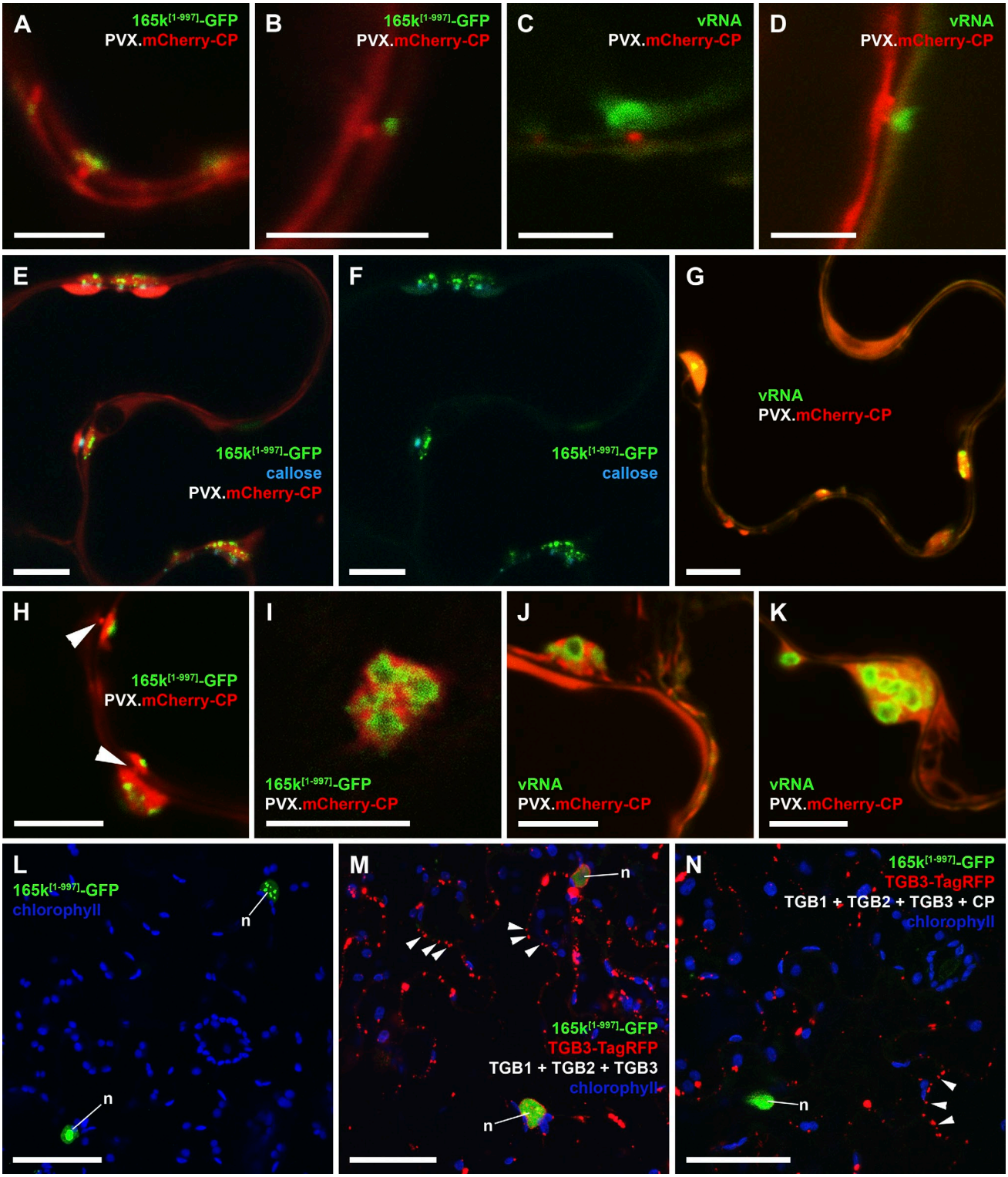

Figure 3. **Localization of replicase and vRNA at PD.** (A and B) At the leading edge of a PVX.mCherry-CP infection 165k[1–997]-GFP is located in punctae next to PD. (C and D) vRNA imaged using PUM-BiFC (Tilsner et al., 2009) shows the same localization. (E and F) One to two cells behind the infection front, mCherry-CP–labeled caps have formed around the 165k[1–997]-GFP granules associated with aniline blue–stained PD. (G) vRNA is also present in punctate hotspots within these caps. (H) mCherry-CP inserted into the PD channel (arrowheads) adjacent to 165[1–997]-GFP–labeled caps. (I) In larger replication bodies, the replicase fusion labels whorls. (J and K) vRNA labels the same whorls in peripheral VRCs. (L) In uninfected cells, 165k[1–997]-GFP localizes to nuclear aggregates (n, nucleus). (M and N) Coexpression of TGB proteins and CP does not alter the localization of replicase in uninfected cells. GFP fluorescence remains confined to the nuclei and is not associated with the TGB3-TagRFP–labeled caps (some of which are indicated by arrowheads). All images are individual z sections except L–N, which are maximum projections of entire z stacks. Bars: (A–D) 5 µm; (E–K) 10 µm; (L–N) 50 µm.

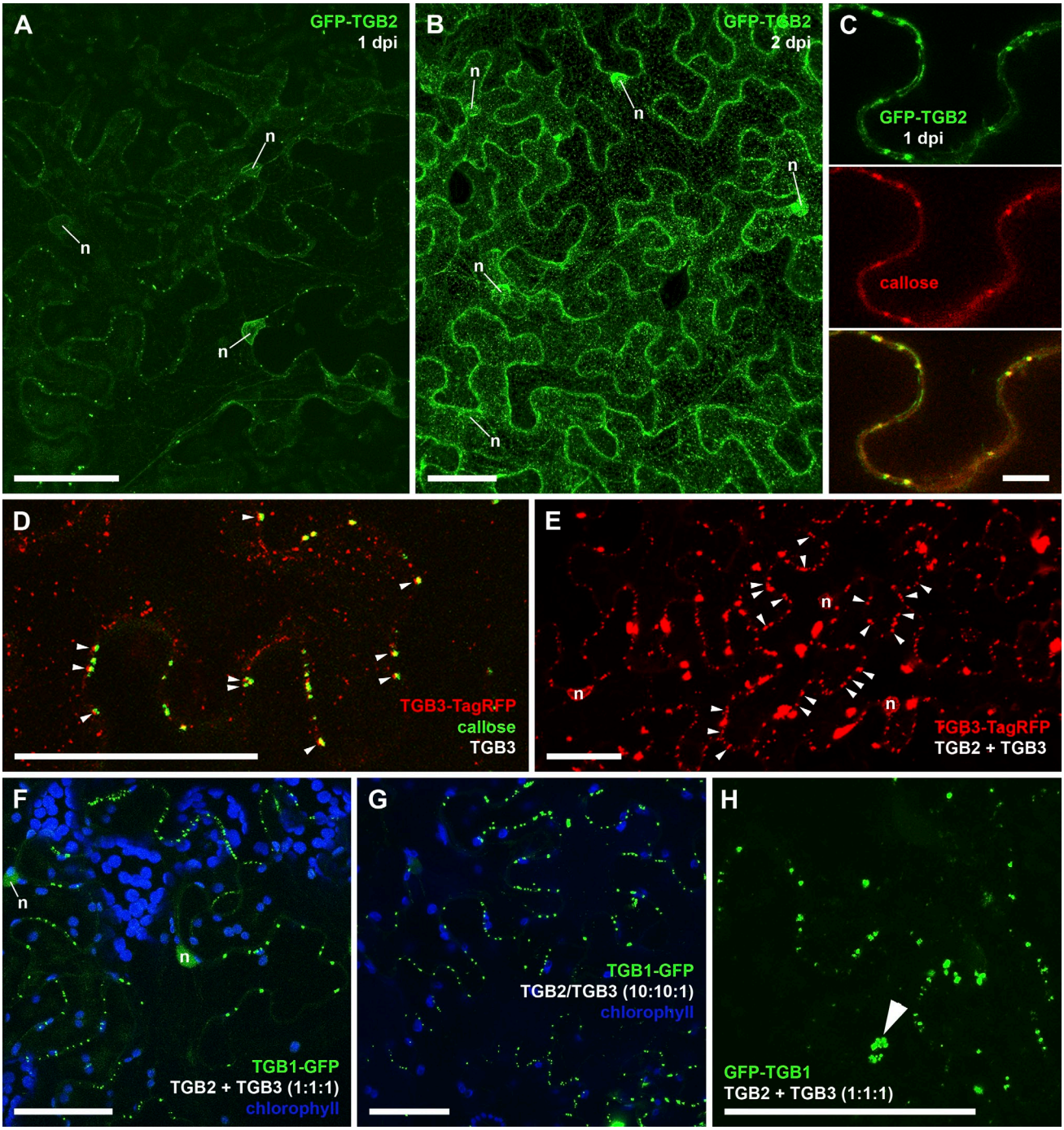

Figure 4. **PD targeting by the TGB2/3 proteins.** White letters indicate coexpression of unfused proteins. (A) At 1 dpi with low expression levels, GFP-TGB2 labels peripheral punctae and the nuclear envelope (n, nucleus). Only faint labeling of tubular ER is visible. (B) At higher expression levels (2 dpi), the ER/nuclear envelope and ER-associated granules are labeled. (C) Colocalization of GFP-TGB2 with aniline blue–stained callose as a PD marker. (top: GFP only; middle: aniline blue only; bottom: merged image). (D) In the presence of unfused TGB3, TGB3-TagRFP labels ER-associated punctae that align with aniline blue–stained PD. (E) Presence of TGB2 significantly increases localization of TGB3-TagRFP to caps (arrowheads; larger TGB3-TagRFP–labeled structures are membrane aggregates). (F and G) Coexpression of TGB2 and 3 from separate plasmids (F) or a bicistronic messenger similar to the viral subgenomic RNA (G) leads to accumulation of TGB1-GFP in PD. (H) N-terminal GFP-TGB1 fusion also recruited to PD by TGB2/3 (arrowhead indicates a pit field at the epidermis–mesophyll interface). In F and G, chloroplast autofluorescence is shown in blue. All images are maximum projections of entire z stacks except C, which is an individual z section. Bars: (A, B, D–H) 50 µm; (C) 10 µm. See also Fig. S2, Fig. S3, and Table S1.

We were also able to reproduce the distinct PD localizations of TGB1 and TGB2/3 in uninfected cells. Combinations of GFP-TGB2 or TGB3-GFP, respectively, in the presence of unfused TGB2 and TGB3 or TGB1, recruited TGB1-TagRFP to PD (Fig. 5, A and B; and Table S1).

TGB2/3 proteins remodel the cortical ER at PD

We next turned to superresolution imaging (3D structured illumination microscopy [3D-SIM]; Fitzgibbon et al., 2010) to obtain clearer images of the TGB2/3 caps associated with PD.

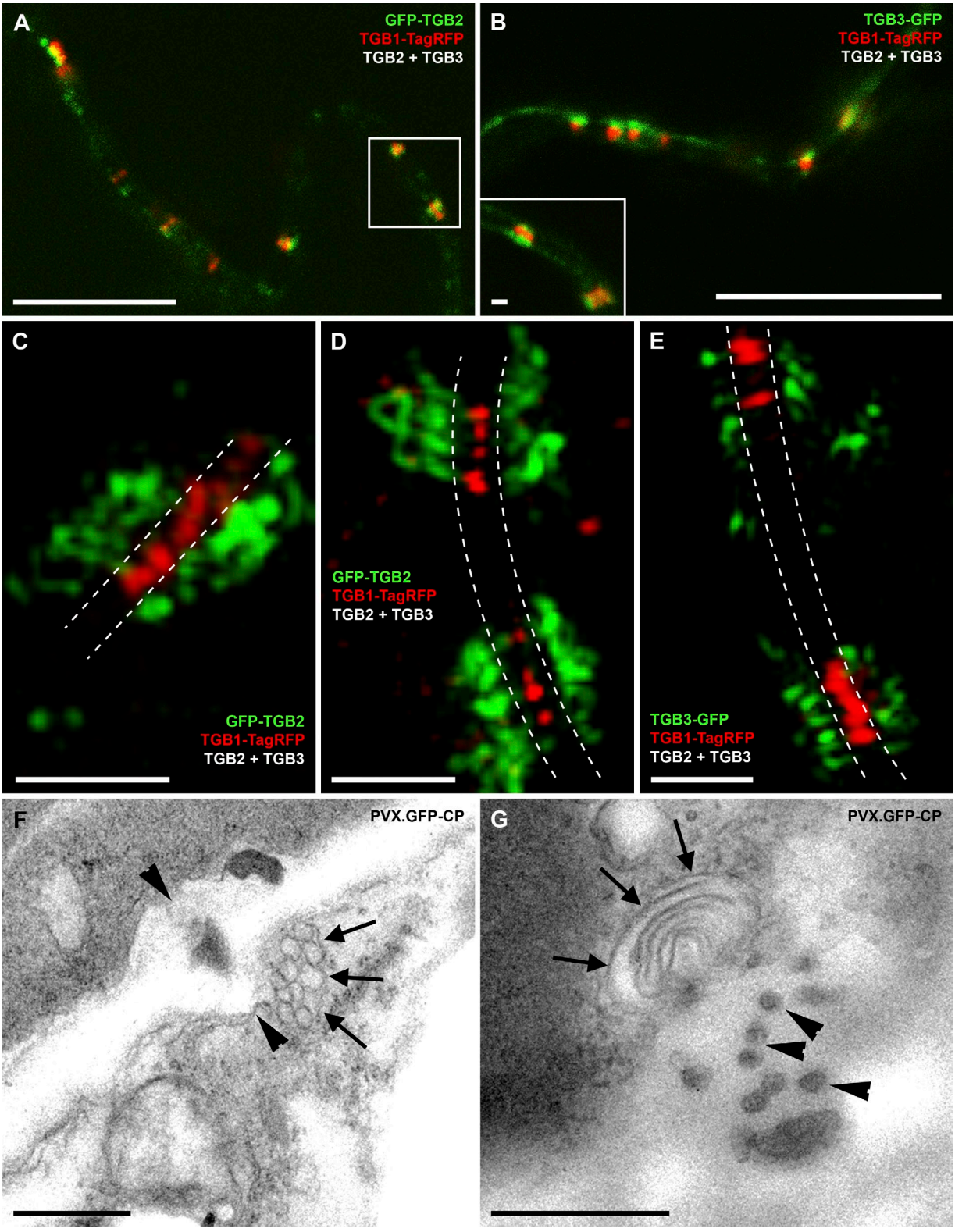

Figure 5. **TGB2/3 remodel the cortical ER at PD.** White letters indicate coexpression of unfused proteins. (A and B) TGB1-TagRFP–labeled PD channels and adjacent caps labeled by GFP-TGB2 (A) and TGB3-GFP (B). Note caps on both sides of PD (boxed area in A and inset in B). (C–E) 3D-SIM super-resolution images showing distinct localization of TGB1-TagRFP in PD channels and GFP-TGB2 (C and D) or TGB3-GFP (E) in cortical ER remodeled into fine membrane loops. Dashed lines indicate the cell wall. (F and G) TEM images of membranous caps (arrows) at PD orifices (arrowheads) at the leading edge of a PVX.GFP-CP infection. The caps appear to be composed either of aggregated vesicles (F) or stacked membrane hoops (G), possibly depending on sectioning angle. Confocal images (A and B) are individual z sections, and 3D-SIM images (C–E) are maximum projections of z stacks. Bars: (A and B, main image) 10 µm; (B [inset] and C–E) 1 µm; (F and G) 500 nm. See also Table S1.

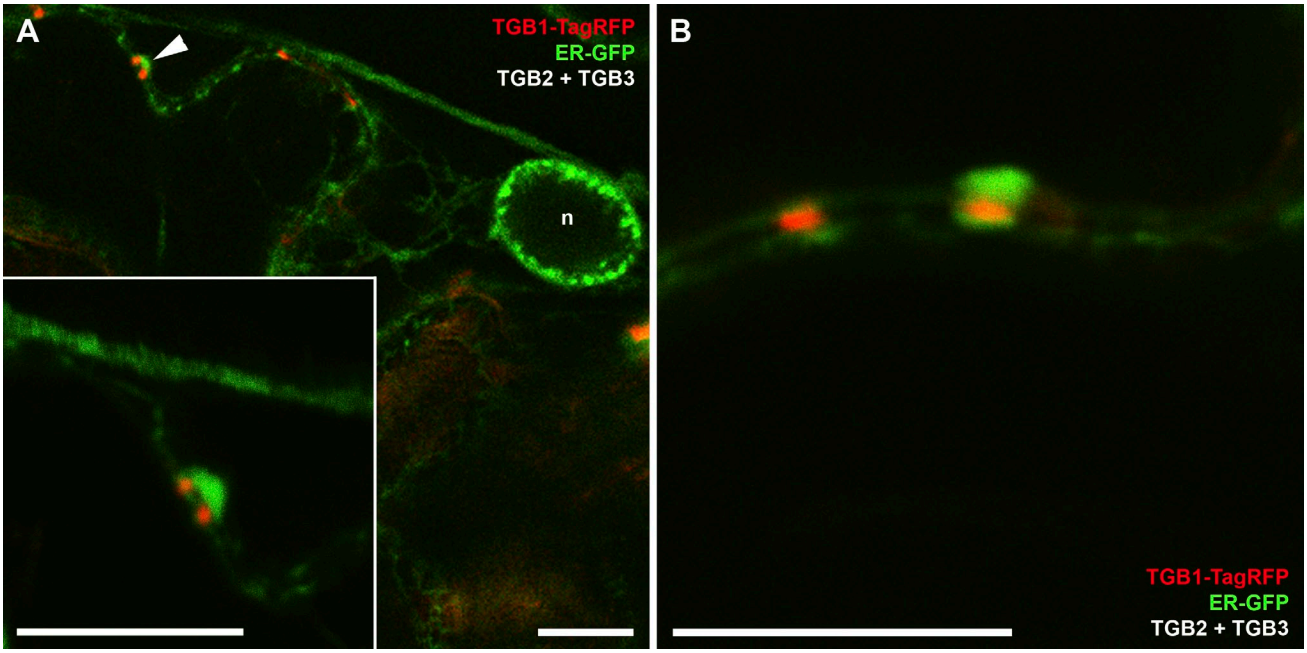

Figure 6. **PD caps are ER derived.** (A and B) PD-associated caps formed in the presence of TGB2/3 and TGB1-TagRFP are labeled by lumenal ER-GFP (Haseloff et al., 1997). The cap marked by an arrowhead in A is magnified in the inset. All images are individual z sections. n, nucleus. Bars, 10 µm.

Using 3D-SIM, we could resolve fine hoops of TGB2-labeled membranes associated with the neck of PD and also observed the spatial separation from TGB1 protein located within the central cavity of PD more clearly (Fig. 5, C and D). The TGB2-labeled membrane hoops resembled TGB2/3-decorated modified ER within PVX perinuclear virus "factories" (Linnik et al., 2013). Identical results were obtained with TGB3 (Fig. 5 E).

To confirm that the modified membrane structures at PD were also present during PVX infection, we also conducted EM. Fluorescent PVX.GFP-CP was used as an infection marker to identify the leading edge for sample preparation. Modified membrane structures, which appeared to be comprised of loops of stacked membranes or accumulated vesicles, were present at PD orifices, confirming the 3D-SIM observations (Fig. 5, F and G). The modified membrane structures were expected to be ER derived because both TGB2 and 3 localize to the ER (Krishnamurthy et al., 2003; Ju et al., 2005). We confirmed this by localizing an ER lumenal marker (Haseloff et al., 1997) to caps formed in the presence of unlabeled TGB2/3 and TGB1-TagRFP–labeled PD (Fig. 6). Collectively, these data show that TGB2/3 induce the formation of remodeled ER membranes at the PD orifices at early infection stages.

TGB1 is required for insertion of CP into PD

Because TGB1 is required for movement, but does not contribute to PD targeting or affect the number or size of TGB2/3 caps (compare Fig. 3 [M and N] and Fig. 4 E), it must have a separate function in virus transport. Intriguingly, at the leading edge of infection, FP-CP was observed only inside the PD channels and not on the cytoplasmic face of the caps (Fig. 2, Fig. 3, and Fig. 4), suggesting that CP is inserted directionally into the PD pore.

Because TGB1 dilates PD (Howard et al., 2004), interacts with CP subunits at the 5′ end of virions (Atabekov et al., 2000; Karpova et al., 2006), and is colocalized with CP inside the pores, it might be required for the insertion of virions into PD. The C terminus of CP and one of the conserved RNA helicase motifs of TGB1, motif IV, are required for their interaction in vitro. PVX CP lacking the C-terminal 10 amino acids (ΔC10) does not interact with TGB1 but can still encapsidate RNA in vitro (Zayakina et al., 2008). We introduced the ΔC10 mutation into a PVX.GFP-CP genome under the control of a 35S promoter (Fig. 1). Agroinfiltration of this construct at very low bacterial OD (OD_{600} = 0.001), as well as microprojectile bombardment experiments, showed that PVX.GFP-CP[ΔC10] was movement deficient (Fig. S3 A). However the virus was clearly infectious, as large perinuclear VRCs were formed (Fig. S3 B). Despite correct targeting of the TGB proteins, the GFP-CP[ΔC10] fusion protein was never observed in PD (Fig. 7 A), as predicted.

To separate TGB PD targeting and CP PD insertion experimentally, and to confirm the role of TGB1 in further detail, we next set up assays to test for movement complementation of a PVX.ΔTGB1.GFP-CP virus (Fig. 1; Tilsner et al., 2012) using ectopically expressed TGB1 variants. Agroinfiltration of 35S::PVX.ΔTGB1.GFP-CP at low OD (OD_{600} = 0.001) results in expression of the mutant virus in isolated cells. To test movement complementation while suppressing potential effects of compromised silencing suppression by TGB1 variants, we co-expressed TGB1 variants and the ectopic silencing suppressor 19k (Voinnet et al., 2003; Bayne et al., 2005). Unfused, wild-type TGB1 fully rescued viral movement, and within 3 dpi, the fluorescent virus covered the entire leaf (Fig. S3 C), also confirming the expression and functionality of the unlabeled protein. Randomly selecting cell boundaries revealed the presence of

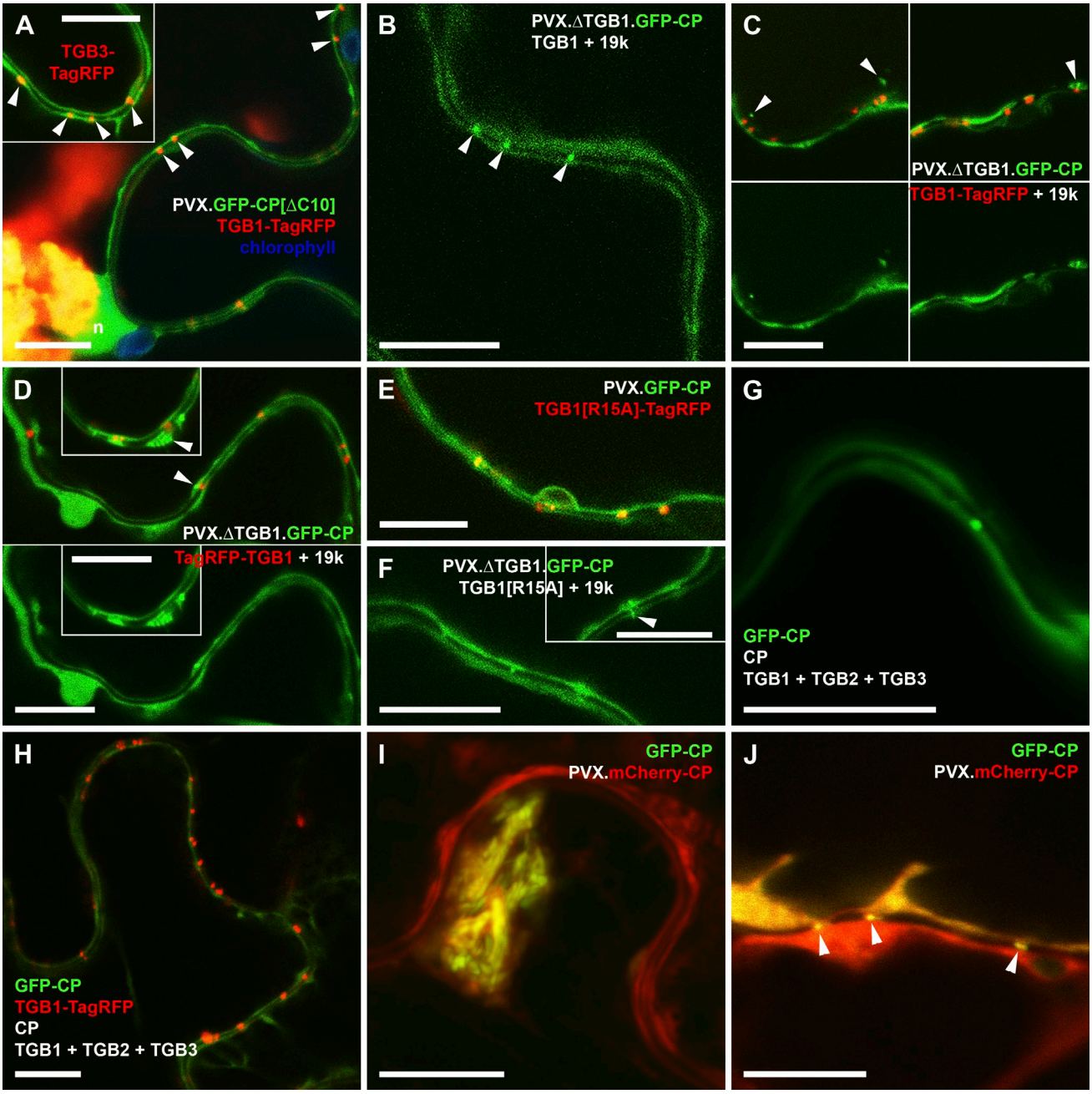

Figure 7. **TGB1 is responsible for insertion of CP into PD.** White letters indicate coexpression of unfused proteins. 19k: ectopic silencing suppressor to compensate for potential effects of suppression deficiency in TGB1 mutants (Voinnet et al., 2003; Bayne et al., 2005). (A) Although TGB1-TagRFP and TGB3-TagRFP (inset) are targeted to PD (arrowheads), GFP-CP[ΔC10], which is defective for TGB1 interaction, is not inserted into the pores. (B) Unfused TGB1 rescues movement of TGB1-deficient PVX. Randomly selected cell–cell interfaces reveals GFP-CP accumulated in PD. Arrowheads highlight GFP-CP inserted into PD. (C) C-terminal TGB1-TagRFP also rescues movement of PVX.ΔTGB1.GFP-CP, but GFP-CP is almost undetectable in PD, although TGB1-TagRFP is normally targeted (top: merged TagRFP and GFP images; bottom: GFP only). Note small packets of GFP-CP virions in the cytoplasm opposite PD (arrowheads), possibly on the cytoplasmic face of (unlabeled) caps. (D) N-terminal TagRFP-TGB1 does not rescue PVX.ΔTGB1.GFP-CP movement, and no GFP-CP is found in PD (top: merged TagRFP and GFP images; bottom: GFP only), but caps containing GFP-CP are visible (inset). Arrowheads highlight packets of GFP-CP stuck outside of PD. (E) TGB1[R15A]-TagRFP is recruited to PD in a PVX.GFP-CP infection. (F) Unfused TGB1[R15A] only partially restores PVX movement, and GFP-CP virion packets appear stuck in caps (inset, arrowhead). In rare cases in which GFP-CP is found in PD, its accumulation is significantly reduced compared with complementation by wild-type TGB1 (compare with B). (G and H) Ectopically expressed GFP-CP does not enter PD in the presence of all three TGB proteins and unfused CP. (I and J) In tissue infected with PVX.mCherry-CP, ectopically expressed GFP-CP is incorporated into virions (I) and found in PD alongside virus-expressed mCherry-CP (arrowheads; J). In A, chloroplast autofluorescence is shown in blue. Images are individual z sections, except I, which is a maximum projection of an entire z stack. Bars, 10 µm. See Fig. S3 for movement phenotypes.

abundant GFP-CP–labeled PD (Fig. 7 B). Previous studies of the ability of N- and C-terminal FP fusions of TGB1 to complement movement have been conflicting (Morozov et al., 1999; Howard et al., 2004; Bayne et al., 2005). In agreement with Bayne et al. (2005), co-infiltration of TGB1-TagRFP resulted in complete restoration of movement (Fig. S3 D), whereas infection sites were still single celled at 3 dpi after co-infiltration of TagRFP-TGB1 (Fig. S3 E). Surprisingly, in both experiments,

GFP-CP accumulation within PD was reduced to the extent that it was virtually undetectable (Fig. 7, C and D), although TGB1-TagRFP complemented virus movement (Fig. S3 D). Because TGB2/3-dependent targeting of TGB1 was fully functional for both fusions, and the only difference to unfused TGB1 was the presence of TGB1 modifications, TGB1 is clearly involved in inserting CP into PD.

Mutational analysis of TGB1

Based on these results, we subsequently tested the ability of several TGB1 mutants for PD recruitment and movement complementation/insertion of CP into PD separately by using FP fused and unfused TGB1 variants, respectively. A TGB1 deletion mutant lacking motif IV required for CP interaction was not recruited to PD (Fig. S4 A), possibly because its overall tertiary structure was too strongly disrupted, and was therefore not tested for movement complementation.

RNA helicase motifs I (Walker A) and II (Walker B) of TGB1 proteins are required for movement of TGB-encoding viruses (Erhardt et al., 2000; Howard et al., 2004; Bayne et al., 2005), but Walker A (GKS to GEA) and B (DEY to RRY) mutants of PVX TGB1 were not recruited to PD (Fig. S4, B and C), and were thus not tested further. However, because ATP (and hence ATPase/RNA helicase activity) is not required for binding of TGB1 to the PVX virion (Atabekov et al., 2000), these mutations are unlikely to be directly related to insertion of CP into PD.

Another TGB1 residue previously implicated in movement is an arginine just upstream of the Walker A motif, which is conserved among TGB1 proteins (Lin et al., 2004; Leshchiner et al., 2006). A TGB1[R15A]-TagRFP fusion was efficiently targeted to PD both in PVX infections and by TGB2/3 (Fig. 7 E and Fig. S5 D). However, the ability of the unfused mutant protein to complement movement of the 35S::PVX.ΔTGB1.GFP-CP virus was strongly reduced. At 3–4 dpi, infection sites resulting from low optical density infiltrations were still small, consisting of ∼10–20 cells (Fig. S3 F). Within these lesions, cell boundaries were mostly devoid of GFP-CP–labeled PD. Instead, small GFP-CP "packets" were sometimes found in or on the cytoplasmic face of caps, as if stuck at the PD orifice (Fig. 7 F, inset). In the few cases in which GFP-CP was found inside PD, fluorescence intensity was greatly reduced compared with the wild-type situation (Fig. 7, F and B). Thus, the TGB1[R15A] mutation significantly affected CP insertion into PD despite effective targeting of TGB1 itself, further confirming that TGB1 functions in directing CP into PD.

Insertion of CP into PD requires the context of viral infection

To test whether TGB1-mediated insertion of GFP-CP into PD requires the context of viral infection, we ectopically coexpressed GFP-CP and all three unfused TGB proteins, as well as unfused CP to mimic the situation in the PVX.GFP-CP overcoat virus in which the fusion protein is partially split (Santa Cruz et al., 1996). GFP-CP had a nucleocytoplasmic distribution and occasionally formed aggregates, but it did not enter PD (Fig. 7, G and H), despite interacting with both TGB1 and TGB2 (Zayakina et al., 2008; Wu et al., 2011). Thus, the TGB-CP protein–protein interactions alone are not sufficient to recruit CP into PD. However, ectopically expressed GFP-CP was incorporated into virions and inserted into PD in tissue infected with PVX.mCherry-CP (Fig. 7, I and J). This strongly indicates that recruitment of CP into PD by TGB1 requires the coordinated assembly of a movement complex, i.e., FP-CP probably enters PD only in association with vRNA.

Discussion

A model for coreplicational insertion of PVX into PD

Although plant and animal RNA viruses both replicate on endomembranes, their movement strategies are entirely different. Animal viruses tend to use exocytic–endocytic pathways for intercellular transport, whereas plant viruses depend exclusively on movement through PD. In this study, we dissected the functions of the TGB proteins during movement of PVX and suggest a revised model for PVX cell-to-cell movement.

All three TGB proteins (as well as CP) are required for movement, but it has remained unclear how they cooperate to facilitate virus transport. TGB2 has been shown to induce the formation of ER-derived granules, which also contain TGB3 and PVX replicase (Ju et al., 2005; Samuels et al., 2007; Bamunusinghe et al., 2009), whereas TGB3 has been implicated in recruiting TGB2 to peripheral bodies (Schepetilnikov et al., 2005). TGB1 dilates PD but does not target them (Howard et al., 2004), and though in other types of TGB-encoding viruses TGB2/3 recruit TGB1 to PD (Erhardt et al., 2000; Verchot-Lubicz et al., 2010), similar evidence has been lacking for potexvirus-type TGB viruses. In this study, we now show that both TGB2 and TGB3 have PD targeting activity and that the peripheral bodies they form consist of reorganized, densely reticulated ER membranes that cap the PD orifice and harbor PVX replication sites. We also show that TGB1, recruited by TGB2/3, is required for inserting CP into the PD channel, probably in the form of a movement complex with vRNA. Collectively, these data suggest a new model of PVX movement, in which replication and cell-to-cell transport are linked at PD entrances.

After establishment of PVX replication complexes on the ER, these become located in ER-derived TGB2/3 granules (Bamunusinghe et al., 2009). The TGB proteins and CP did not affect the localization of $165k^{[1–997]}$-GFP in uninfected cells, and its recruitment to PD caps required a full infection, i.e., the presence of full-length replicase, vRNA, virus-recruited host factors, or a combination of these. Together with the association of ribosomes with the granules (Ju et al., 2005) and the requirement of replication for the synthesis of subgenomic TGB messenger RNAs, this suggests that the TGB proteins are translated locally near replication complexes and then remain associated with them through a network of interactions between replicase, vRNA, TGBs, and CP (Zayakina et al., 2008; Lee et al., 2010, 2011; Wu et al., 2011). TGB-associated replication complexes will rapidly encounter PD orifices because the ER surface is highly motile and continuous through PD (Tilsner et al., 2011). At PD, they become anchored by TGB2/3.

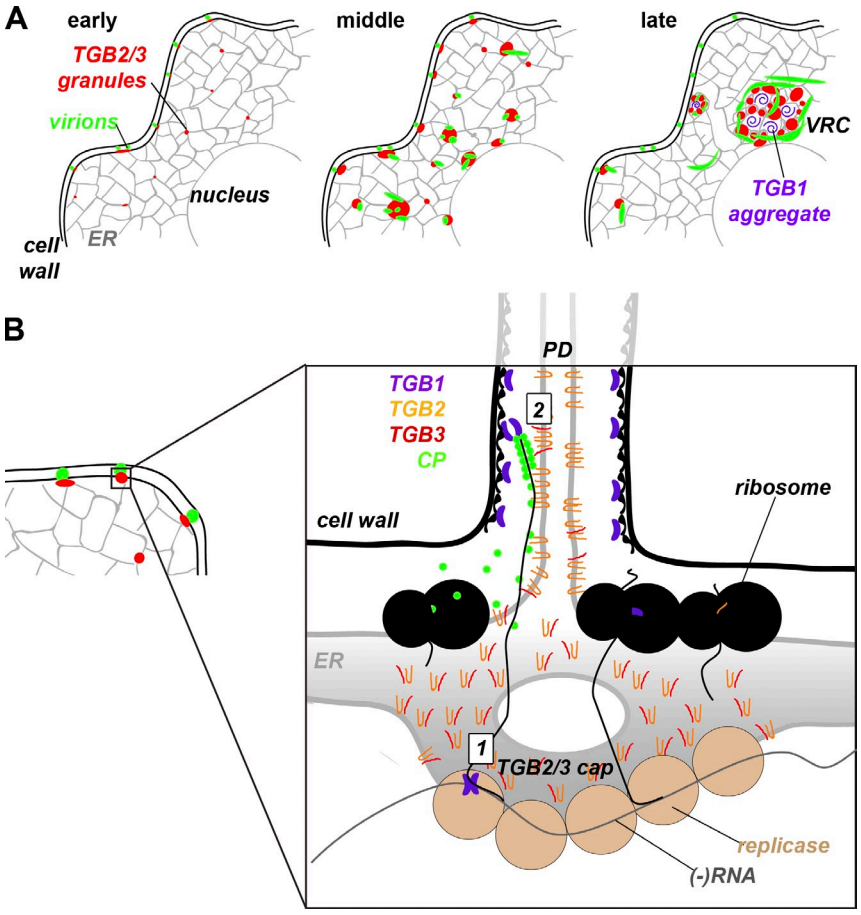

Figure 8. **Model for coreplicational insertion of PVX into PD.** (A) Development of PVX replication sites: At early infection stages, TGB2/3-associated replication complexes are motile on the ER network. Some become anchored at PD for delivery of virus into the pores. Later, replication sites grow into PD-associated caps and ER-associated granules, respectively. Finally, the TGB2/3 granules accumulate in a perinuclear VRC around TGB1 aggregates (Tilsner et al., 2012). (B) At PD caps (approximately to scale), TGB2/3 have remodeled the ER adjacent to a PD entrance and anchored a VRC. They have also entered the ER tubule within the PD pore. Viral RNA emerging from the replicase is diverted toward movement, possibly with the aid of the RNA helicase TGB1 (boxed 1). The nascent vRNA begins immediate encapsidation. TGB1 binds to the partially encapsidated virion and directs it into PD (boxed 2). See Discussion for details.

Within PD, the desmotubule is a unique ER membrane domain with extreme tubular constriction, requiring the presence of membrane-bending proteins, such as reticulons (Tilsner et al., 2011). Potexviral TGB3 localizes preferentially to high-curvature, reticulon-containing ER domains (Lee et al., 2010; Wu et al., 2011), and the TGB2/3 transmembrane complex may interact with PD-specific ER proteins for PD targeting and anchoring (Tilsner et al., 2011).

Through gradual accumulation of vRNA and gene products, the anchored replication complexes develop into PD caps, whereas those that remain unanchored on the ER grow into the motile granules (Fig. 8 A). Previous immunolocalizations failed to detect PVX replicase at PD (Bamunusinghe et al., 2009), but this may have been a result of the low number of naturally occurring epitopes. In our ectopic expression approach, additional replicase molecules may have been recruited to the PD caps, increasing the signal. Definite proof of replication within the PD caps would require the localization of (−) RNA or double-stranded RNA intermediates, an approach that is currently unfeasible at the necessary subcellular resolution. However, in agreement with our model, callose-enclosed (a plant defense mechanism) vesicles and virus particles were previously found at PD entrances in EM micrographs of mature PVX infections and probably represent late stages of the PD-anchored replication sites (Allison and Shalla, 1974).

At the PD caps, the RNA helicase activity of TGB1 functions in diverting progeny vRNA away from replication and translation toward assembly of movement complexes (Fig. 8 B, boxed 1; Tilsner and Oparka, 2012). Because of the 5′ → 3′ directionality of RNA synthesis, the 5′ end of the viral genome emerges first from the replicase. The 5′-terminal 107 nucleotides of PVX are required for movement (Lough et al., 2006) and contain a stem loop structure involved in the initiation of potexvirus encapsidation (Kwon et al., 2005; Verchot-Lubicz et al., 2007). In the presence of locally translated CP, nascent progeny RNA may be encapsidated in cis. TGB1 binds specifically to the 5′ end of partially or fully encapsidated virions, where the CP C terminus is exposed (Karpova et al., 2006; Zayakina et al., 2008). By interacting with both CP and PD, TGB1 could then direct the nascent virus particle into the gated PD pore (Fig. 8 B, boxed 2). TGB2, which binds RNA, CP, and TGB1 (Hsu et al., 2009; Wu et al., 2011) as well as contributing to gating (Angell et al., 1996; Tamai and Meshi, 2001), may also be involved in inserting the virus into PD.

Coreplicational insertion into PD from localized replication sites would explain the directionality of GFP-CP insertion from the caps. The sequence specificity of the PVX replicase (Plante et al., 2000) and viral encapsidation could provide specificity to the movement process. Interaction between CP and replicase is also required for movement (Lee et al., 2011) and might contribute to coreplicational encapsidation and PD insertion. Although localized replication at PD does not exclude the possibility that vRNA is trafficked from replication complexes elsewhere in the cell, localization of TGB2 at PD before the

appearance of ER-associated granules suggests that the PD orifice is the first port of call for replication.

Coreplicational intercellular RNA transport represents a new form of subcellular compartmentation of RNA metabolism and differs from the spatially separated replication and movement found in animal RNA viruses (den Boon et al., 2010). However, it bears resemblance to the nuclear export of cellular mRNAs, which can be spatially coupled to transcription (Rodríguez-Navarro and Hurt, 2011) and requires the action of specific RNA helicases (Ledoux and Guthrie, 2011). Furthermore, it is likely that spatial and functional coupling of replication and movement is common among RNA plant viruses.

Implications for movement of other RNA plant viruses

MPs of other filamentous plant viruses also interact asymmetrically with the 5′ end of virions (Peremyslov et al., 2004; Gabrenaite-Verkhovskaya et al., 2008), suggesting a similar mode of PD insertion, and may replicate at PD (see Fig. 5 III in Wei et al., 2010). The model virus, Tobacco mosaic virus (TMV), which has a single MP and moves as a nonencapsidated MP–vRNA complex, probably also replicates at PD (Szécsi et al., 1999; Kawakami et al., 2004). Spatially linked replication and movement may thus be more widespread among plant viruses than previously thought.

The TMV MP can complement PVX movement (Fedorkin et al., 2001), and movement trans-complementation is widespread among plant viruses (Latham and Wilson, 2008). Therefore, interactions between MPs and the replication machinery cannot be very specific. Recruitment of replication complexes to PD may be mediated by interactions of locally translated MPs with vRNA or CPs or with host factors commonly usurped for virus replication (Tilsner and Oparka, 2012). Several host proteins commonly identified in replication complexes, including DnaJ-type chaperones, Hsp70 family heat shock proteins, and the translation initiation factor eIF4E, have also been characterized as MP interactors or directly implicated in movement (Gao et al., 2004; Robaglia and Caranta, 2006; Serva and Nagy, 2006; Hofius et al., 2007; Shimizu et al., 2009; Krenz et al., 2010; Nagy et al., 2011).

Coreplicational delivery of vRNA into PD could maximize the efficiency of PD delivery and viral concentration gradients across PD during early infection and could also confer movement specificity for viruses that move in nonencapsidated forms. An even more intriguing possibility is that coupling of replication and movement plays a role in regulating the cellular MOI. Plant virus infections often exhibit viral exclusion, i.e., the first viral genomes that enter a cell prevent further superinfections. The MOI is in the order of units (~1–15), and it is likely that viruses actively regulate it to optimize gene copy numbers and recombination rates (Gutiérrez et al., 2012). This may require co-transport of replication machinery through PD, suggested for both PVX and TMV (Kawakami et al., 2004; Lee et al., 2011), and could be the main reason for coreplicational virus transport. Thus, coreplicational movement of plant viruses may directly link RNA processing to viral epidemiology.

Materials and methods

Constructs

Standard cloning procedures were followed. Primers are listed in Table S2. The virus constructs PVX.GFP-CP (Santa Cruz et al., 1996), PVX.pum-mCherry-CP (referred to as PVX.mCherry-CP throughout the Results; Tilsner et al., 2009), carrying modified cDNAs of the PVX genome under control of a *T7* promoter, and the binary construct 35S::PVX.ΔTGB1.GFP-CP (Tilsner et al., 2012) have been previously described. The binary vector 35S::PVX.GFP-CP was generated by excising the GFP-CP cassette from PVX.GFP-CP as an EagI(blunted)–SpeI fragment and ligating it into AscI(blunted)–SpeI-treated 35S::PVX.GFP (pGR106.GFP; Jones et al., 1999). To make 35S::PVX.GFP-CP[ΔC10], a fragment of PVX.GFP-CP from the unique XhoI site within the *CP* ORF to the SpeI site downstream of the PVX 3′UTR was amplified, and the deletion of the C-terminal 10 amino acids of *CP* was introduced by overlap PCR with primers dC10 reverse and dC10 forward (Table S2). The PCR product was T/A cloned into pGEM-T Easy (Promega). After sequence verification, the XhoI–SpeI fragment containing part of *GFP*, the *CP[ΔC10]* mutated ORF, and the PVX 3′UTR was ligated into XhoI–SpeI-treated 35S::PVX.GFP-CP to generate 35S::PVX.GFP-CP[ΔC10].

Expression vectors for transient expression of each individual PVX TGB protein either unfused or N- or C-terminally fused to a FP were constructed using pGWB402Ω (unfused), pGWB405 (C-terminal GFP), pGWB406 (N-terminal GFP), pGWB460 (C-terminal TagRFP), and pGWB461 (N-terminal TagRFP) Gateway vectors (Nakagawa et al., 2007) and have been previously described (Tilsner et al., 2012). N- and C-terminal fusions and unfused expression are indicated in all figures and throughout this paper. A bicistronic construct encompassing the *TGB2* and *TGB3* ORFs was generated by amplification with primers attB-TGB2 forward and attB-TGB3 reverse (Table S2). The TGB1[ΔIV], TGB1[GKS to GEA], TGB1[DEY to RRY], and TGB1[R15A] mutants were generated by overlap PCR mutagenesis with the respective primers listed in Table S2. TGB1[ΔIV] lacks amino acid residues 113–122 of the wild-type protein. The TGB PCR products were recombined into the pDONR207 vector using Gateway recombinase (Invitrogen). Sequenced inserts were recombined into the appropriate pGWB vectors for unfused expression or N- or C-terminal fusion. PVX replicase, truncated replicase, and CP were amplified from PVX.GFP-CP and Gateway cloned into pGWB405, pGWB406, and pGWB402Ω, respectively, for GFP-fused and unfused expression.

The construction of the PUM-BiFC RNA imaging system was described in Tilsner et al. (2009, 2012). In brief, monomeric (A206K) Citrine YFP ORF was split between amino acids 173 and 174. The N-terminal fragment was translationally fused to the N terminus of a modified HsPumilio1 RNA binding domain (PUMHD3794; N971S, H972N, and Q975E), which binds nucleotides 3,794–3,801 of the TMV genome. The C-terminal Citrine fragment was fused to the C terminus of modified PUMHD3809 (S863N, C935S, Q939E, N971C, C1007N, and N1043C), which binds nucleotides 3,809–3,816 of TMV. Fusion proteins were assembled in pGEM-T Easy, subcloned into pENTR1A (Invitrogen), and Gateway recombined into pGWB402Ω (Nakagawa et al., 2007) for *Agrobacterium tumefaciens*–mediated plant expression. The TMV 3,974–3,816 recognition sequence was cloned into a PVX vector expressing an mCherry-CP fusion (PVX.pum-mChery-CP; Tilsner et al., 2009). The plasmid pBIN.19k, which expresses the Tomato bushy stunt virus 19k silencing suppressor under the control of a 35S promoter, was described in Voinnet et al. (2003).

Plant material and inoculations

All infections and transient expression were performed on *Nicotiana benthamiana* plants grown at 20°C with a 16 h/8 h light/dark cycle. T7 polymerase in vitro transcription of PVX cDNA clones with an mMessage mMachine kit (Ambion/Applied Biosystems) and leaf inoculation were as previously described in Santa Cruz et al. (1998). PVX was passaged by homogenizing ~0.5 × 0.5–cm pieces of fresh or frozen infected tissue in 100 µl H_2O and rub inoculating 5–10 µl of this sap on aluminum oxide–dusted leaves. For colocalizations of virally and ectopically expressed FP fusions, transient expression constructs were agroinfiltrated 2–3 d after virus inoculation. For movement complementation assays, TGB constructs and 35S::PVX constructs were co-infiltrated simultaneously.

For agroinfiltration, strain AGL1 agrobacteria were electroporated with the relevant binary plasmids and stored as −80°C glycerol stocks. Agrobacteria cultures were grown in Luria and Bertani medium with appropriate antibiotics at 28°C for 2 d, pelleted, and resuspended in infiltration medium (10 mM MES, 10 mM $MgCl_2$, and 15 µM acetosyringone; Voinnet et al., 2003). After 1-h incubation in the dark, *A. tumefaciens* suspensions were diluted to an appropriate optical density: OD_{600} was 0.5

for individual, 0.25 each for combinations of two, 0.2 each for three, and 0.15 each for combinations of four or more co-infiltrated constructs. Infiltration was via the abaxial surface using a needle-less syringe. To test for cell-to-cell movement of modified 35S::PVX constructs, agrobacteria were infiltrated at an OD_{600} of 0.001, which results in transient transformation of mostly individual cells and low numbers of groups of two to four adjacent transformed cells. In movement complementation assays, the ectopic silencing suppressor 19k was co-infiltrated at an OD_{600} of 0.25 to compensate for potential compromised suppressor activity of the TGB1 mutants (Voinnet et al., 2003; Bayne et al., 2005).

For transient transformation of individual epidermal cells by microprojectile bombardment, 2–5 µg plasmid DNA was $CaCl_2$ precipitated onto 1.25 mg of 1-µm gold particles (Bio-Rad Laboratories) and resuspended in 100 µl ethanol. 5-µl aliquots were bombarded onto detached *N. benthamiana* leaves using a biolistic particle delivery system (PDS-1000/He; Bio-Rad Laboratories) at 1,100 psi with 6 cm between the leaf surface and the stopping grid. Leaves were kept with their petiole in water until imaging (Tilsner et al., 2009).

Light microscopy

Confocal imaging was performed at room temperature 1–4 d after agroinfiltrations to observe localizations at the lowest detectable limit as well as after stronger expression. Whole leaves, half leaves, or ∼2 × 2–cm leaf pieces were removed from plants and mounted with the lower epidermis facing up onto glass microscope slides using double-sided sticky tape (Banner, Ltd.). For staining of PD-associated callose, 0.1 mg/ml aniline blue solution in water was infiltrated into leaves immediately before imaging.

All confocal imaging was performed on an upright confocal microscope (SP2; Leica). HCX Apochromat 63×/numerical aperture 0.90 water U-V-1 and HCX Apochromat 40×/numerical aperture 0.40 water U-V-1 water-dipping lenses were used for all subcellular localizations, and an HCX Apochromat 20×/numerical aperture 0.50 water U-V-1 water-dipping lens was used for imaging of entire viral lesions. Lenses were immersed in a drop of water placed directly on the plant sample. Excitation wavelengths were as follows: aniline blue, 405 nm; GFP, 488 nm; mCitrine (PUM-BiFC), 514 nm; TagRFP, 561 nm; and mCherry, 594 nm. Detection ranges were optimized for each fluorophore combination to minimize bleed through, and where necessary, sequential scanning was used. Microscope power settings were adjusted to optimize contrast for each individual image. Images were collected using LCS software (Leica) and imported into Photoshop (Adobe) for brightness and contrast adjustments and assembly of composite figures for publication.

For 3D-SIM superresolution imaging, epidermal peels of leaves expressing desired fluorescent fusion constructs were aldehyde fixed for 30–45 min at room temperature. After fixation, they were assembled on a coverslip, mounted in antifade medium (Citifluor AF1; Agar Scientific), and sealed with nail varnish (Linnik et al., 2013). 3D-SIM imaging was performed at room temperature on an inverted microscope (OMX version 2; Applied Precision) using a U Plan S Apochromat 100×, numerical aperture 1.4, oil-immersion objective lens (Olympus), and a back-illuminated 512 × 512 electron multiplying charge-coupled device camera (Cascade II; Photometrics) as previously described in Fitzgibbon et al. (2010) and Linnik et al. (2013). GFP was excited at 488 nm, and TagRFP was excited at 594 nm. Laser light was scrambled by passing through a diffraction grating to generate the structured illumination by interference of light orders in the image plane to create a 3D sinusoidal pattern, with lateral stripes ∼0.2 µm apart. The pattern was shifted through five lateral phases and three angular rotations for each z section, separated by 0.125 µm. Raw images were processed and reconstructed to reveal structures with greater resolution. Green and red channels were aligned using predetermined shifts measured with fluorescent microbeads. See Fitzgibbon et al. (2010) for further details.

EM

Tissue infected with PVX.GFP-CP was identified by GFP fluorescence, excised from the leaves, and fixed in glutaraldehyde. For standard transmission EM (TEM), fixation was in 4% glutaraldehyde followed by postfix in 2% osmium tetroxide and embedding in Araldite. For immuno-EM, samples were fixed in 5% glutaraldehyde without postfixing and embedded in Araldite (Roberts, 1994). Anti-TGB2 antibody was obtained by immunizing a rabbit with N-terminally His_6-tagged TGB2 expressed in *Escherichia coli* BL21 (DE3) pLysS cells from a pET32a vector (EMD Millipore) and purified by denaturing Ni-affinity chromatography. Goat anti–rabbit IgG (heavy and light chains) conjugated to 15-nm gold (GE Healthcare) was used as the secondary antibody (Roberts, 1994; Oparka et al., 1996). After immunogold labeling, samples were counterstained with uranyl acetate and lead citrate. Electron micrographs were obtained on a transmission electron microscope (BioTwin CM120; Philips).

Online supplemental material

Fig. S1 shows control experiments for TGB1 localizations. Fig. S2 shows control experiments for TGB3 localizations. Fig. S3 shows movement phenotypes of CP and TGB1 mutants. Fig. S4 shows localizations of TGB1 mutants. Table S1 summarizes localizations of all TGB combinations. Table S2 lists primers used in this study. Online supplemental material is available at http://www.jcb.org/cgi/content/full/jcb.201304003/DC1. Additional data are available in the JCB DataViewer at http://dx.doi.org/10.1083/jcb.201304003.dv.

We thank K. Bell and S. Mitchell for help with TEM samples and M. Posch for help with 3D-SIM microscopy. We thank Prof. L. Torrance (The James Hutton Institute, Dundee, and University of St Andrews) for use of her laboratory and access to James Hutton Institute confocal microscopes during parts of the project.

The work was funded by Biotechnology and Biological Sciences Research Council grant BB/H018719/1 to K.J. Oparka and J. Tilsner.

Submitted: 1 April 2013
Accepted: 16 May 2013

References

Allison, A.V., and T.A. Shalla. 1974. The ultrastructure of local lesions induced by potato virus X: a sequence of cytological events in the course of infection. *Phytopathology*. 64:784–793. http://dx.doi.org/10.1094/Phyto-64-784

Angell, S.M., C. Davies, and D.C. Baulcombe. 1996. Cell-to-cell movement of potato virus X is associated with a change in the size-exclusion limit of plasmodesmata in trichome cells of *Nicotiana clevelandii*. *Virology*. 216:197–201. http://dx.doi.org/10.1006/viro.1996.0046

Atabekov, J.G., N.P. Rodionova, O.V. Karpova, S.V. Kozlovsky, and V.Y. Poljakov. 2000. The movement protein-triggered *in situ* conversion of potato virus X virion RNA from a nontranslatable into a translatable form. *Virology*. 271:259–263. http://dx.doi.org/10.1006/viro.2000.0319

Bamunusinghe, D., C.L. Hemenway, R.S. Nelson, A.A. Sanderfoot, C.M. Ye, M.A.T. Silva, M. Payton, and J. Verchot-Lubicz. 2009. Analysis of potato virus X replicase and TGBp3 subcellular locations. *Virology*. 393:272–285. http://dx.doi.org/10.1016/j.virol.2009.08.002

Bayne, E.H., D.V. Rakitina, S.Y. Morozov, and D.C. Baulcombe. 2005. Cell-to-cell movement of potato potexvirus X is dependent on suppression of RNA silencing. *Plant J.* 44:471–482. http://dx.doi.org/10.1111/j.1365-313X.2005.02539.x

Chapman, S., G. Hills, J. Watts, and D. Baulcombe. 1992. Mutational analysis of the coat protein gene of potato virus X: effects on virion morphology and viral pathogenicity. *Virology*. 191:223–230. http://dx.doi.org/10.1016/0042-6822(92)90183-P

den Boon, J.A., A. Diaz, and P. Ahlquist. 2010. Cytoplasmic viral replication complexes. *Cell Host Microbe*. 8:77–85. http://dx.doi.org/10.1016/j.chom.2010.06.010

Doronin, S.V., and C. Hemenway. 1996. Synthesis of potato virus X RNAs by membrane-containing extracts. *J. Virol.* 70:4795–4799.

Erhardt, M., M. Morant, C. Ritzenthaler, C. Stussi-Garaud, H. Guilley, K. Richards, G. Jonard, S. Bouzoubaa, and D. Gilmer. 2000. P42 movement protein of Beet necrotic yellow vein virus is targeted by the movement proteins P13 and P15 to punctate bodies associated with plasmodesmata. *Mol. Plant Microbe Interact.* 13:520–528. http://dx.doi.org/10.1094/MPMI.2000.13.5.520

Fedorkin, O.N., A.G. Solovyev, N.E. Yelina, A.A. Zamyatnin Jr., R.A. Zinovkin, K. Mäkinen, J. Schiemann, and S. Yu Morozov. 2001. Cell-to-cell movement of potato virus X involves distinct functions of the coat protein. *J. Gen. Virol.* 82:449–458.

Fitzgibbon, J., K. Bell, E. King, and K. Oparka. 2010. Super-resolution imaging of plasmodesmata using three-dimensional structured illumination microscopy. *Plant Physiol.* 153:1453–1463. http://dx.doi.org/10.1104/pp.110.157941

Gabrenaite-Verkhovskaya, R., I.A. Andreev, N.O. Kalinina, L. Torrance, M.E. Taliansky, and K. Mäkinen. 2008. Cylindrical inclusion protein of potato virus A is associated with a subpopulation of particles isolated from infected plants. *J. Gen. Virol.* 89:829–838. http://dx.doi.org/10.1099/vir.0.83406-0

Gao, Z., E. Johansen, S. Eyers, C.L. Thomas, T.H. Noel Ellis, and A.J. Maule. 2004. The potyvirus recessive resistance gene, sbm1, identifies a novel

role for translation initiation factor eIF4E in cell-to-cell trafficking. *Plant J.* 40:376–385. http://dx.doi.org/10.1111/j.1365-313X.2004.02215.x

Gutiérrez, S., Y. Michalakis, and S. Blanc. 2012. Virus population bottlenecks during within-host progression and host-to-host transmission. *Curr. Opin. Virol*. 2:546–555. http://dx.doi.org/10.1016/j.coviro.2012.08.001

Haseloff, J., K.R. Siemering, D.C. Prasher, and S. Hodge. 1997. Removal of a cryptic intron and subcellular localization of green fluorescent protein are required to mark transgenic *Arabidopsis* plants brightly. *Proc. Natl. Acad. Sci. USA*. 94:2122–2127. http://dx.doi.org/10.1073/pnas.94.6.2122

Hofius, D., A.T. Maier, C. Dietrich, I. Jungkunz, F. Börnke, E. Maiss, and U. Sonnewald. 2007. Capsid protein-mediated recruitment of host DnaJ-like proteins is required for Potato virus Y infection in tobacco plants. *J. Virol.* 81:11870–11880. http://dx.doi.org/10.1128/JVI.01525-07

Howard, A.R., M.L. Heppler, H.J. Ju, K. Krishnamurthy, M.E. Payton, and J. Verchot-Lubicz. 2004. *Potato virus X* TGBp1 induces plasmodesmata gating and moves between cells in several host species whereas CP moves only in *N. benthamiana* leaves. *Virology*. 328:185–197. http://dx.doi.org/10.1016/j.virol.2004.06.039

Hsu, H.T., Y.H. Tseng, Y.L. Chou, S.H. Su, Y.H. Hsu, and B.Y. Chang. 2009. Characterization of the RNA-binding properties of the triple-gene-block protein 2 of Bamboo mosaic virus. *Virol. J.* 6:50. http://dx.doi.org/10.1186/1743-422X-6-50

Jones, L., A.J. Hamilton, O. Voinnet, C.L. Thomas, A.J. Maule, and D.C. Baulcombe. 1999. RNA-DNA interactions and DNA methylation in post-transcriptional gene silencing. *Plant Cell*. 11:2291–2301.

Ju, H.-J., T.D. Samuels, Y.-S. Wang, E. Blancaflor, M. Payton, R. Mitra, K. Krishnamurthy, R.S. Nelson, and J. Verchot-Lubicz. 2005. The potato virus X TGBp2 movement protein associates with endoplasmic reticulum-derived vesicles during virus infection. *Plant Physiol.* 138:1877–1895. http://dx.doi.org/10.1104/pp.105.066019

Kalinina, N.O., D.V. Rakitina, A.G. Solovyev, J. Schiemann, and S.Yu. Morozov. 2002. RNA helicase activity of the plant virus movement proteins encoded by the first gene of the triple gene block. *Virology*. 296:321–329. http://dx.doi.org/10.1006/viro.2001.1328

Karpova, O.V., O.V. Zayakina, M.V. Arkhipenko, E.V. Sheval, O.I. Kiselyova, V.Y. Poljakov, I.V. Yaminsky, N.P. Rodionova, and J.G. Atabekov. 2006. Potato virus X RNA-mediated assembly of single-tailed ternary 'coat protein-RNA-movement protein' complexes. *J. Gen. Virol.* 87:2731–2740. http://dx.doi.org/10.1099/vir.0.81993-0

Kawakami, S., Y. Watanabe, and R.N. Beachy. 2004. Tobacco mosaic virus infection spreads cell to cell as intact replication complexes. *Proc. Natl. Acad. Sci. USA*. 101:6291–6296. http://dx.doi.org/10.1073/pnas.0401221101

Krenz, B., V. Windeisen, C. Wege, H. Jeske, and T. Kleinow. 2010. A plastid-targeted heat shock cognate 70kDa protein interacts with the Abutilon mosaic virus movement protein. *Virology*. 401:6–17. http://dx.doi.org/10.1016/j.virol.2010.02.011

Krishnamurthy, K., M. Heppler, R. Mitra, E. Blancaflor, M. Payton, R.S. Nelson, and J. Verchot-Lubicz. 2003. The Potato virus X TGBp3 protein associates with the ER network for virus cell-to-cell movement. *Virology*. 309:135–151. http://dx.doi.org/10.1016/S0042-6822(02)00102-2

Kwon, S.J., M.R. Park, K.W. Kim, C.A. Plante, C.L. Hemenway, and K.H. Kim. 2005. *cis*-Acting sequences required for coat protein binding and in vitro assembly of Potato virus X. *Virology*. 334:83–97. http://dx.doi.org/10.1016/j.virol.2005.01.018

Latham, J.R., and A.K. Wilson. 2008. Transcomplementation and synergism in plants: implications for viral transgenes? *Mol. Plant Pathol.* 9:85–103.

Ledoux, S., and C. Guthrie. 2011. Regulation of the Dbp5 ATPase cycle in mRNP remodeling at the nuclear pore: a lively new paradigm for DEAD-box proteins. *Genes Dev.* 25:1109–1114. http://dx.doi.org/10.1101/gad.2062611

Lee, C.C., Y.N. Ho, R.H. Hu, Y.T. Yen, Z.C. Wang, Y.C. Lee, Y.H. Hsu, and M. Meng. 2011. The interaction between bamboo mosaic virus replication protein and coat protein is critical for virus movement in plant hosts. *J. Virol.* 85:12022–12031. http://dx.doi.org/10.1128/JVI.05595-11

Lee, S.-C., C.-H. Wu, and C.-W. Wang. 2010. Traffic of a viral movement protein complex to the highly curved tubules of the cortical endoplasmic reticulum. *Traffic*. 11:912–930. http://dx.doi.org/10.1111/j.1600-0854.2010.01064.x

Leshchiner, A.D., A.G. Solovyev, S.Y. Morozov, and N.O. Kalinina. 2006. A minimal region in the NTPase/helicase domain of the TGBp1 plant virus movement protein is responsible for ATPase activity and cooperative RNA binding. *J. Gen. Virol.* 87:3087–3095. http://dx.doi.org/10.1099/vir.0.81971-0

Leshchiner, A.D., E.A. Minina, D.V. Rakitina, V.K. Vishnichenko, A.G. Solovyev, S.Yu. Morozov, and N.O. Kalinina. 2008. Oligomerization of the potato virus X 25-kD movement protein. *Biochemistry (Mosc.)*. 73:50–55. http://dx.doi.org/10.1134/S0006297908010070

Lin, M.K., B.Y. Chang, J.T. Liao, N.S. Lin, and Y.H. Hsu. 2004. Arg-16 and Arg-21 in the N-terminal region of the triple-gene-block protein 1 of Bamboo mosaic virus are essential for virus movement. *J. Gen. Virol.* 85:251–259. http://dx.doi.org/10.1099/vir.0.19442-0

Linnik, O., J. Liesche, J. Tilsner, and K.J. Oparka. 2013. Unraveling the structure of viral replication complexes at super-resolution. *Front Plant Sci*. 4:6. http://dx.doi.org/10.3389/fpls.2013.00006

Lough, T.J., R.H. Lee, S.J. Emerson, R.L.S. Forster, and W.J. Lucas. 2006. Functional analysis of the 5′ untranslated region of potexvirus RNA reveals a role in viral replication and cell-to-cell movement. *Virology*. 351:455–465. http://dx.doi.org/10.1016/j.virol.2006.03.043

Lucas, W.J. 2006. Plant viral movement proteins: agents for cell-to-cell trafficking of viral genomes. *Virology*. 344:169–184. http://dx.doi.org/10.1016/j.virol.2005.09.026

Morozov, S.Y., and A.G. Solovyev. 2003. Triple gene block: modular design of a multifunctional machine for plant virus movement. *J. Gen. Virol.* 84:1351–1366. http://dx.doi.org/10.1099/vir.0.18922-0

Morozov, S.Y., A.G. Solovyev, N.O. Kalinina, O.N. Fedorkin, O.V. Samuilova, J. Schiemann, and J.G. Atabekov. 1999. Evidence for two nonoverlapping functional domains in the potato virus X 25K movement protein. *Virology*. 260:55–63. http://dx.doi.org/10.1006/viro.1999.9788

Nagy, P.D., R.Y. Wang, J. Pogany, A. Hafren, and K. Mäkinen. 2011. Emerging picture of host chaperone and cyclophilin roles in RNA virus replication. *Virology*. 411:374–382. http://dx.doi.org/10.1016/j.virol.2010.12.061

Nakagawa, T., T. Suzuki, S. Murata, S. Nakamura, T. Hino, K. Maeo, R. Tabata, T. Kawai, K. Tanaka, Y. Niwa, et al. 2007. Improved Gateway binary vectors: high-performance vectors for creation of fusion constructs in transgenic analysis of plants. *Biosci. Biotechnol. Biochem.* 71:2095–2100. http://dx.doi.org/10.1271/bbb.70216

Oparka, K.J., A.G. Roberts, I.M. Roberts, D.A.M. Prior, and S. Santa Cruz. 1996. Viral coat protein is targeted to, but does not gate, plasmodesmata during cell-to-cell movement of potato virus X. *Plant J.* 10:805–813. http://dx.doi.org/10.1046/j.1365-313X.1996.10050805.x

Peremyslov, V.V., I.A. Andreev, A.I. Prokhnevsky, G.H. Duncan, M.E. Taliansky, and V.V. Dolja. 2004. Complex molecular architecture of beet yellows virus particles. *Proc. Natl. Acad. Sci. USA*. 101:5030–5035. http://dx.doi.org/10.1073/pnas.0400303101

Plante, C.A., K.H. Kim, N. Pillai-Nair, T.A.M. Osman, K.W. Buck, and C.L. Hemenway. 2000. Soluble, template-dependent extracts from *Nicotiana benthamiana* plants infected with potato virus X transcribe both plus- and minus-strand RNA templates. *Virology*. 275:444–451. http://dx.doi.org/10.1006/viro.2000.0512

Robaglia, C., and C. Caranta. 2006. Translation initiation factors: a weak link in plant RNA virus infection. *Trends Plant Sci.* 11:40–45. http://dx.doi.org/10.1016/j.tplants.2005.11.004

Roberts, I.M. 1994. Factors affecting the efficiency of immunogold labelling of plant virus antigens in thin sections. *J. Virol. Methods*. 50:155–166. http://dx.doi.org/10.1016/0166-0934(94)90172-4

Rodionova, N.P., O.V. Karpova, S.V. Kozlovsky, O.V. Zayakina, M.V. Arkhipenko, and J.G. Atabekov. 2003. Linear remodeling of helical virus by movement protein binding. *J. Mol. Biol.* 333:565–572. http://dx.doi.org/10.1016/j.jmb.2003.08.058

Rodríguez-Navarro, S., and E. Hurt. 2011. Linking gene regulation to mRNA production and export. *Curr. Opin. Cell Biol.* 23:302–309. http://dx.doi.org/10.1016/j.ceb.2010.12.002

Samuels, T.D., H.-J. Ju, C.-M. Ye, C.M. Motes, E.B. Blancaflor, and J. Verchot-Lubicz. 2007. Subcellular targeting and interactions among the *Potato virus X* TGB proteins. *Virology*. 367:375–389. http://dx.doi.org/10.1016/j.virol.2007.05.022

Santa Cruz, S., S. Chapman, A.G. Roberts, I.M. Roberts, D.A.M. Prior, and K.J. Oparka. 1996. Assembly and movement of a plant virus carrying a green fluorescent protein overcoat. *Proc. Natl. Acad. Sci. USA*. 93:6286–6290. http://dx.doi.org/10.1073/pnas.93.13.6286

Santa Cruz, S., A.G. Roberts, D.A.M. Prior, S. Chapman, and K.J. Oparka. 1998. Cell-to-cell and phloem-mediated transport of potato virus X. The role of virions. *Plant Cell*. 10:495–510.

Schepetilnikov, M.V., U. Manske, A.G. Solovyev, A.A. Zamyatnin Jr., J. Schiemann, and S.Yu. Morozov. 2005. The hydrophobic segment of Potato virus X TGBp3 is a major determinant of the protein intracellular trafficking. *J. Gen. Virol.* 86:2379–2391. http://dx.doi.org/10.1099/vir.0.80865-0

Schoelz, J.E., P.A. Harries, and R.S. Nelson. 2011. Intracellular transport of plant viruses: finding the door out of the cell. *Mol Plant*. 4:813–831. http://dx.doi.org/10.1093/mp/ssr070

Serva, S., and P.D. Nagy. 2006. Proteomics analysis of the tombusvirus replicase: Hsp70 molecular chaperone is associated with the replicase and enhances viral RNA replication. *J. Virol.* 80:2162–2169. http://dx.doi.org/10.1128/JVI.80.5.2162-2169.2006

Shimizu, T., A. Yoshii, K. Sakurai, K. Hamada, Y. Yamaji, M. Suzuki, S. Namba, and T. Hibi. 2009. Identification of a novel tobacco DnaJ-like protein that interacts with the movement protein of tobacco mosaic virus. *Arch. Virol.* 154:959–967. http://dx.doi.org/10.1007/s00705-009-0397-6

Solovyev, A.G., T.A. Stroganova, A.A. Zamyatnin Jr., O.N. Fedorkin, J. Schiemann, and S.Yu. Morozov. 2000. Subcellular sorting of small membrane-associated triple gene block proteins: TGBp3-assisted targeting of TGBp2. *Virology*. 269:113–127. http://dx.doi.org/10.1006/viro.2000.0200

Szécsi, J., X.S. Ding, C.O. Lim, M. Bendahmane, M.J. Cho, R.S. Nelson, and R.N. Beachy. 1999. Development of Tobacco mosaic virus infection sites in *Nicotiana benthamiana. Mol. Plant Microbe Interact.* 12:143–152. http://dx.doi.org/10.1094/MPMI.1999.12.2.143

Tamai, A., and T. Meshi. 2001. Cell-to-cell movement of *Potato virus X:* the role of p12 and p8 encoded by the second and third open reading frames of the triple gene block. *Mol. Plant Microbe Interact.* 14:1158–1167. http://dx.doi.org/10.1094/MPMI.2001.14.10.1158

Tilsner, J., and K.J. Oparka. 2012. Missing links? - The connection between replication and movement of plant RNA viruses. *Curr Opin Virol*. 2:705–711. http://dx.doi.org/10.1016/j.coviro.2012.09.007

Tilsner, J., O. Linnik, N.M. Christensen, K. Bell, I.M. Roberts, C. Lacomme, and K.J. Oparka. 2009. Live-cell imaging of viral RNA genomes using a Pumilio-based reporter. *Plant J.* 57:758–770. http://dx.doi.org/10.1111/j.1365-313X.2008.03720.x

Tilsner, J., K. Amari, and L. Torrance. 2011. Plasmodesmata viewed as specialised membrane adhesion sites. *Protoplasma*. 248:39–60. http://dx.doi.org/10.1007/s00709-010-0217-6

Tilsner, J., O. Linnik, K.M. Wright, K. Bell, A.G. Roberts, C. Lacomme, S. Santa Cruz, and K.J. Oparka. 2012. The TGB1 movement protein of Potato virus X reorganizes actin and endomembranes into the X-body, a viral replication factory. *Plant Physiol.* 158:1359–1370. http://dx.doi.org/10.1104/pp.111.189605

Tseng, Y.-H., H.-T. Hsu, Y.-L. Chou, C.-C. Hu, N.-S. Lin, Y.-H. Hsu, and B.-Y. Chang. 2009. The two conserved cysteine residues of the triple gene block protein 2 are critical for both cell-to-cell and systemic movement of *Bamboo mosaic virus. Mol. Plant Microbe Interact.* 22:1379–1388. http://dx.doi.org/10.1094/MPMI-22-11-1379

Verchot-Lubicz, J., C.M. Ye, and D. Bamunusinghe. 2007. Molecular biology of potexviruses: recent advances. *J. Gen. Virol.* 88:1643–1655. http://dx.doi.org/10.1099/vir.0.82667-0

Verchot-Lubicz, J., L. Torrance, A.G. Solovyev, S.Y. Morozov, A.O. Jackson, and D. Gilmer. 2010. Varied movement strategies employed by triple gene block-encoding viruses. *Mol. Plant Microbe Interact.* 23:1231–1247. http://dx.doi.org/10.1094/MPMI-04-10-0086

Voinnet, O., C. Lederer, and D.C. Baulcombe. 2000. A viral movement protein prevents spread of the gene silencing signal in *Nicotiana benthamiana. Cell*. 103:157–167. http://dx.doi.org/10.1016/S0092-8674(00)00095-7

Voinnet, O., S. Rivas, P. Mestre, and D. Baulcombe. 2003. An enhanced transient expression system in plants based on suppression of gene silencing by the p19 protein of tomato bushy stunt virus. *Plant J.* 33:949–956. http://dx.doi.org/10.1046/j.1365-313X.2003.01676.x

Wei, T., C. Zhang, J. Hong, R. Xiong, K.D. Kasschau, X. Zhou, J.C. Carrington, and A. Wang. 2010. Formation of complexes at plasmodesmata for potyvirus intercellular movement is mediated by the viral protein P3N-PIPO. *PLoS Pathog.* 6:e1000962. http://dx.doi.org/10.1371/journal.ppat.1000962

Wu, C.H., S.C. Lee, and C.W. Wang. 2011. Viral protein targeting to the cortical endoplasmic reticulum is required for cell–cell spreading in plants. *J. Cell Biol.* 193:521–535. http://dx.doi.org/10.1083/jcb.201006023

Zayakina, O., M. Arkhipenko, S. Kozlovsky, N. Nikitin, A. Smirnov, P. Susi, N. Rodionova, O. Karpova, and J. Atabekov. 2008. Mutagenic analysis of potato virus X movement protein (TGBp1) and the coat protein (CP): in vitro TGBp1-CP binding and viral RNA translation activation. *Mol. Plant Pathol.* 9:37–44.